Supplementary Information

Microfluidic control of axonal guidance

*(Revised for **Scientific Reports**)*

Ling Gu[1†], Bryan Black[1†], Simon Ordonez[1], Argha Mondal[1‡], Ankur Jain[2] and Samarendra Mohanty[1*]

[1]Biophysics and Physiology Lab, Department of Physics,

[2]Department of Mechanical and Aerospace Engineering,

University of Texas at Arlington, TX 76019.

†co-first authors

‡Present address: Dept of Physics, IISER-Kolkata, India

* To whom correspondence should be addressed.

Dr. Samarendra Mohanty, Biophysics and Physiology Group,
Department of Physics, University of Texas at Arlington,
502 Yates Street, 108 Science Hall, Arlington, TX 76019, USA.
Email smohanty@uta.edu,
Tel. 817-272-1177. Fax: +1-817-272-3637.

Supplementary Methods:

Theoretical Calculation of axon bending:

One of the best methods used nowadays to solve boundary value problems is to divide the object of interest into small pieces, which are called finite elements and use polynomials (shape functions) to obtain approximated solutions. Here we use the same Finite Element Method (FEM) for structural analysis of a neuron under fluid flow pressure. Our axon-bending problem can be governed by three equations expressed as follows:

Kinematic relationship: $\kappa(x) = -\frac{d^2 w(x)}{dx^2}$;

Constitutional law: $M(x) = D(x)\kappa(x)$;

And equilibrium equation: $\frac{d^2 M(x)}{dx^2} = -f(x)$

Where x is the coordinate along the axon length. $w(x)$ is the deflection of axon from its initial position, $\kappa(x)$ is the generalized strain of the curvature of deformation, and $M(x)$ is bending moment in the axon, where $D(x) = E(x)J(x)$ is the flexural rigidity of the axon. $E(x)$ is Young's modulus, and $J(x)$ is the moment of inertia of the axon along its cross-section. $f(x)$ is the distributed force acting on the axon due to fluid flow. Combining those equations we get the net displacement based equilibrium equation for the bending axon: $\frac{d^2}{dx^2}\left[D(x)\frac{d^2 w}{dx^2} \right] = f(x)$

Lets say the axonal shaft is now divided into number of small elements, where its two node points x_i and x_{i+1} define the ith element. Assuming the deflection of the ith element to be cubic polynomial:

$w(\xi) = a_0 + a_1\xi + a_2\xi^2 + a_3\xi^3$, where $\xi = 2x \Big/ \left(x_{i+1} - x_i\right) - \left(x_{i+1} + x_i\right) \Big/ \left(x_{i+1} - x_i\right)$ is the local coordinate of the ith element. Now considering the boundary conditions i.e. at the fixed end of the axon (the point after which the axon does not feel any force due to fluid flow) $w = 0, dw/dx = 0$, and at the free end $M = \bar{M}, dM/dx = \bar{Q}$, where $\bar{M}$ is the bending moment and $\bar{Q}$ is the shear force respectively, we obtain the interpolation from of the final equilibrium deformation as follows:

$w(\xi) = N_1(\xi)w_i + N_2(\xi)\theta_i + N_3(\xi)w_{i+1} + N_4(\xi)\theta_{i+1}$

Where,

$$N_1(\xi)=\frac{1}{4}(\xi-1)^2(\xi+2);\ N_2(\xi)=\frac{1}{4}(\xi-1)^2(\xi+1);$$

$$N_3(\xi)=\frac{1}{4}(\xi+1)^2(-\xi+2);\ N_4(\xi)=\frac{1}{4}(\xi+1)^2(\xi-1)$$

These are called Hermite polynomials. In matrix form they can be written as $w(\xi)=N(\xi)\delta$, where:

$$\delta=[\ w_i \quad \theta_{i+1} \quad w_i \quad \theta_{i+1}\ ]^T;$$

$$N(\xi)=\begin{bmatrix} N_1(\xi) & N_2(\xi) & N_3(\xi) & N_4(\xi) \end{bmatrix}.$$

The global finite element equilibrium equation of the axonal shaft can be written in a compact form as, $[K]*\{W\}=\{F\}$, where:

$$[K]=\begin{pmatrix} 12 & 6l & -12 & 6l \\ 6l & 4l^2 & -6l & 2l^2 \\ -12 & -6l & 12 & -6l \\ 6l & 2l^2 & -6l & 4l^2 \end{pmatrix}$$

$\{W\}$ is the global nodal displacement vector of the deformed axon, and $\{F\}$ is the force or moment matrix, where l is half length of each element.

The algorithm follows as:

1. Enter the flexural rigidity, axon length and the maximum force applied at the tip of the axon.
2. Find out the element stiffness matrix and assemble that into global stiffness matrix.
3. Remove the first and second row and column of the reduced global stiffness matrix to incorporate the boundary condition as the angular and displacements are constrained on the first node, as there is attachment of axonal shaft with the surface.
4. After obtaining the reduced stiffness matrix and the force matrix, multiply the inverse of the reduced stiffness matrix and force matrix to obtain the displacements.
5. Calculate the shape functions and using the nodal displacements of the axonal shaft, find the displacements along the elements and plot the displacements to obtain the deflection of the axonal shaft.
6. Calculate the radius of curvature of the deformed axonal shaft. Plot with different number of microtubules and decreasing applied forces.

Supplementary Figure captions:

Suppl. Figure 1. (a) Microfluidic guidance setup. M: folding mirror; MO: microscopic objective; HAL: halogen lamp; CON: condenser; SC: sample chamber; Microsyringe nanopump to introduce microfluidic flow to sample chamber. (b) Percentage of axons following along and against the direction of microfluidic flow. Also shown is the percentage of axons maintaining its original direction in spite of microfluidic flow and the percentage of retracted and detached axons.

Suppl. Figure 2. (a) The effect of different rates of fluid flow on the force induced on the axon. (b) Fluid flow induced integrated force on the axons of different diameters.

Suppl. Figure 3. Response of neuronal growth cone against the microfluidic flow. (a to i) Time-lapse images of turning of growth cone against the direction of microfluidic flow (marked by red arrow). The angle between original growth direction and flow direction is ~140^0. Scale bar: 20 μm

Suppl. Figure 4. Time-lapse (10 min) images showing response of growth cone to application of microfluidic flow. (a) Axon turning downward, (b) retraction bulb formation upon microfluidic flow application (direction of flow is marked by white arrow). (c) Retraction of axon, (d) fusion of axonal bulbs, (e) emergence of growth cone, (f) turning of axon along direction of flow.

Suppl. Figure 5. (a) Simulation of flow-force induced bending radius as a function of number of microtubules in an axon. (b) Simulated bending angle as a function of number of microtubules for fixed fluid-force. (c) Sequence of overlay profiles depicting the direction of axonal growth with 5 min-intervals.

Suppl. Figure 6. (a-d) Slight retraction and no directional response observed due to microfluidic flow. (e-f) Complete detachment of axons due to microfluidic flow. The direction of the fluid flow is indicated by red arrows. All scale bars represent 15 μm.

Supplementary video caption:

Suppl. Movie 1. Turning and fasciculation of axonal growth cone by microfluidic flow.

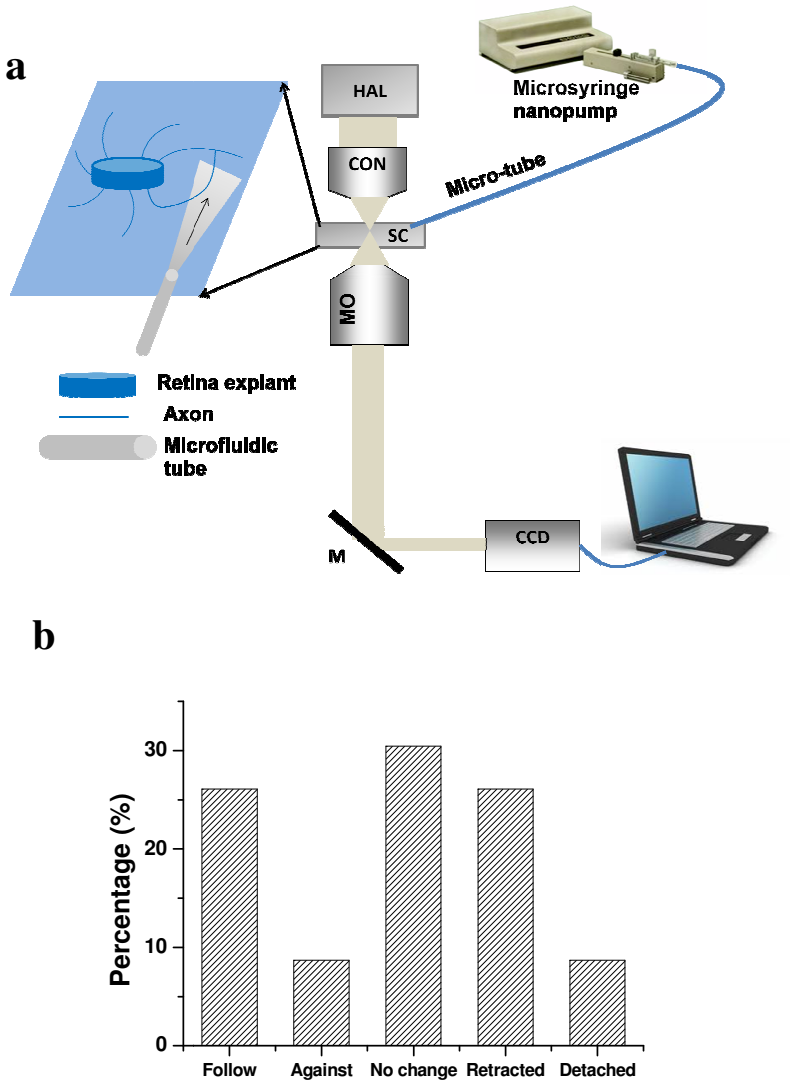

Suppl. Figure 1. (a) Microfluidic guidance setup. M: folding mirror; MO: microscopic objective; HAL: halogen lamp; CON: condenser; SC: sample chamber; Microsyringe nanopump to introduce microfluidic flow to sample chamber. (b) Percentage of axons following along and against the direction of microfluidic flow. Also shown is the percentage of axons maintaining its original direction in spite of microfluidic flow and the percentage of retracted and detached axons.

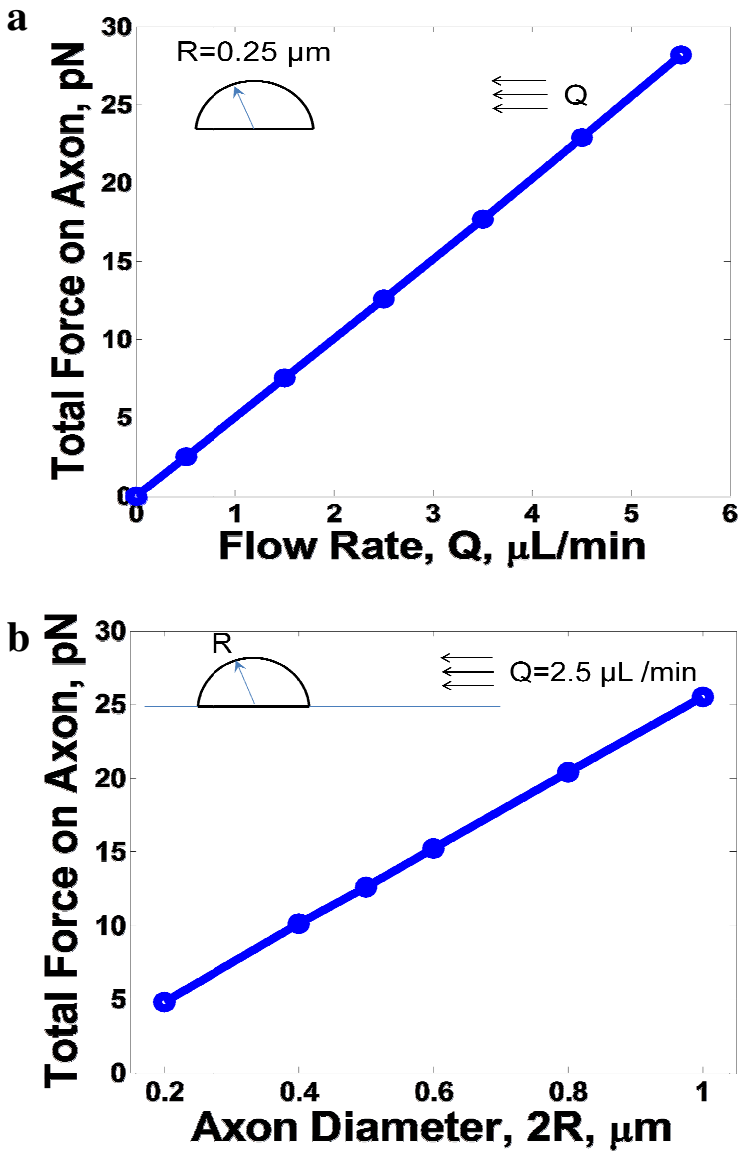

Suppl. Figure 2. (a) The effect of different rates of fluid flow on the force induced on the axon. (b) Fluid flow induced integrated force on the axons of different diameters.

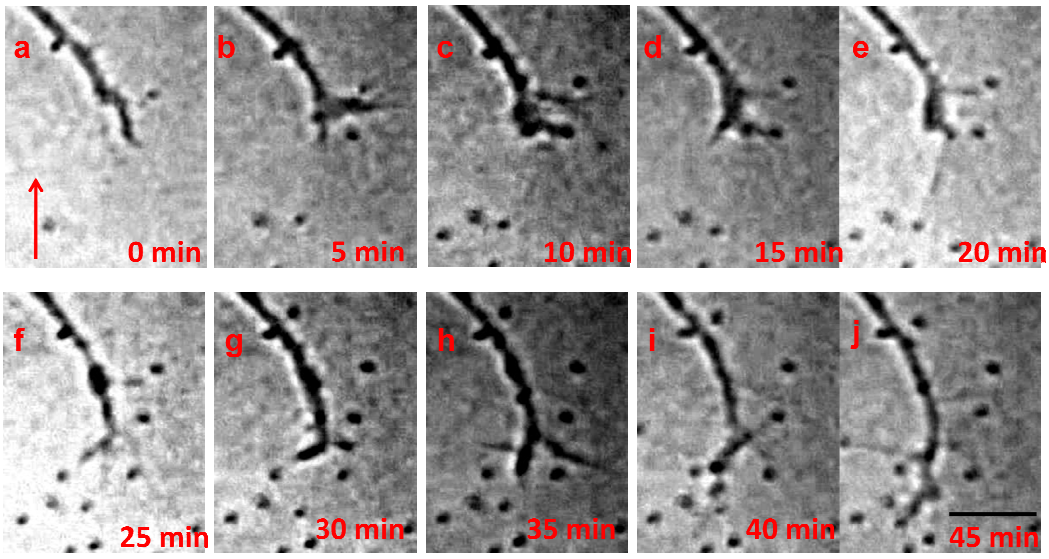

Suppl. Figure 3. Response of neuronal growth cone against the microfluidic flow. (a to i) Time-lapse images of turning of growth cone against the direction of microfluidic flow (marked by red arrow). The angle between original growth direction and flow direction is ~140^0. Scale bar: 20 µm

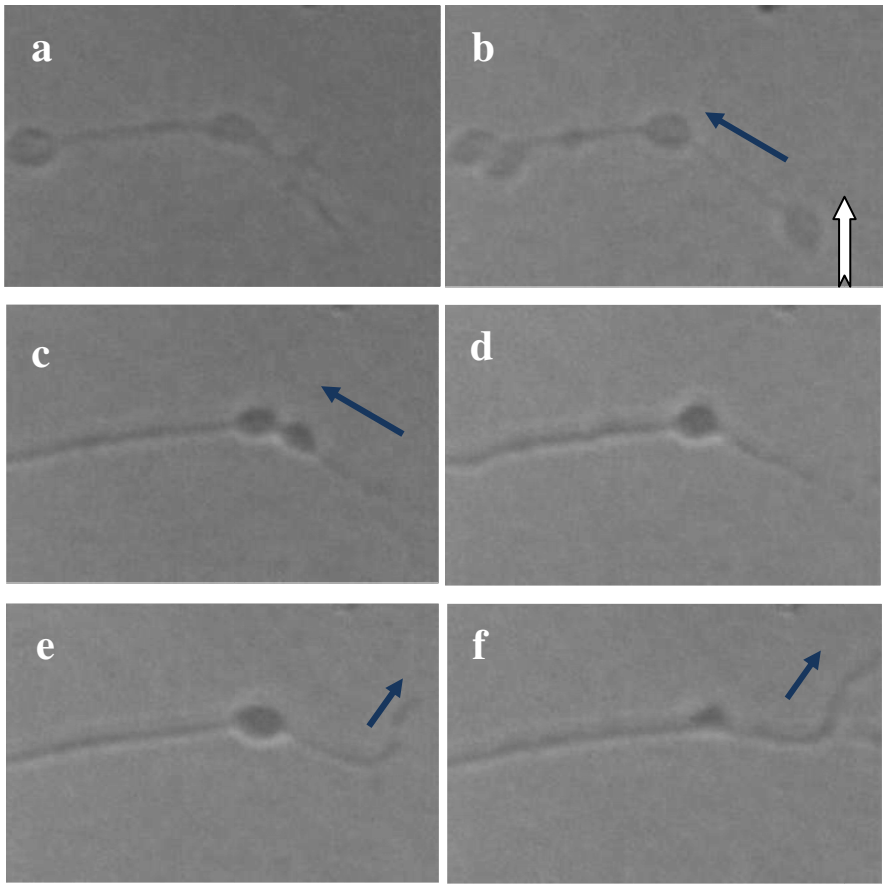

Suppl. Figure 4. Time-lapse (10 min) images showing response of growth cone to application of microfluidic flow. (a) Axon turning downward, (b) retraction bulb formation upon microfluidic flow application (direction of flow is marked by white arrow). (c) Retraction of axon, (d) fusion of axonal bulbs, (e) emergence of growth cone, (f) turning of axon along direction of flow.

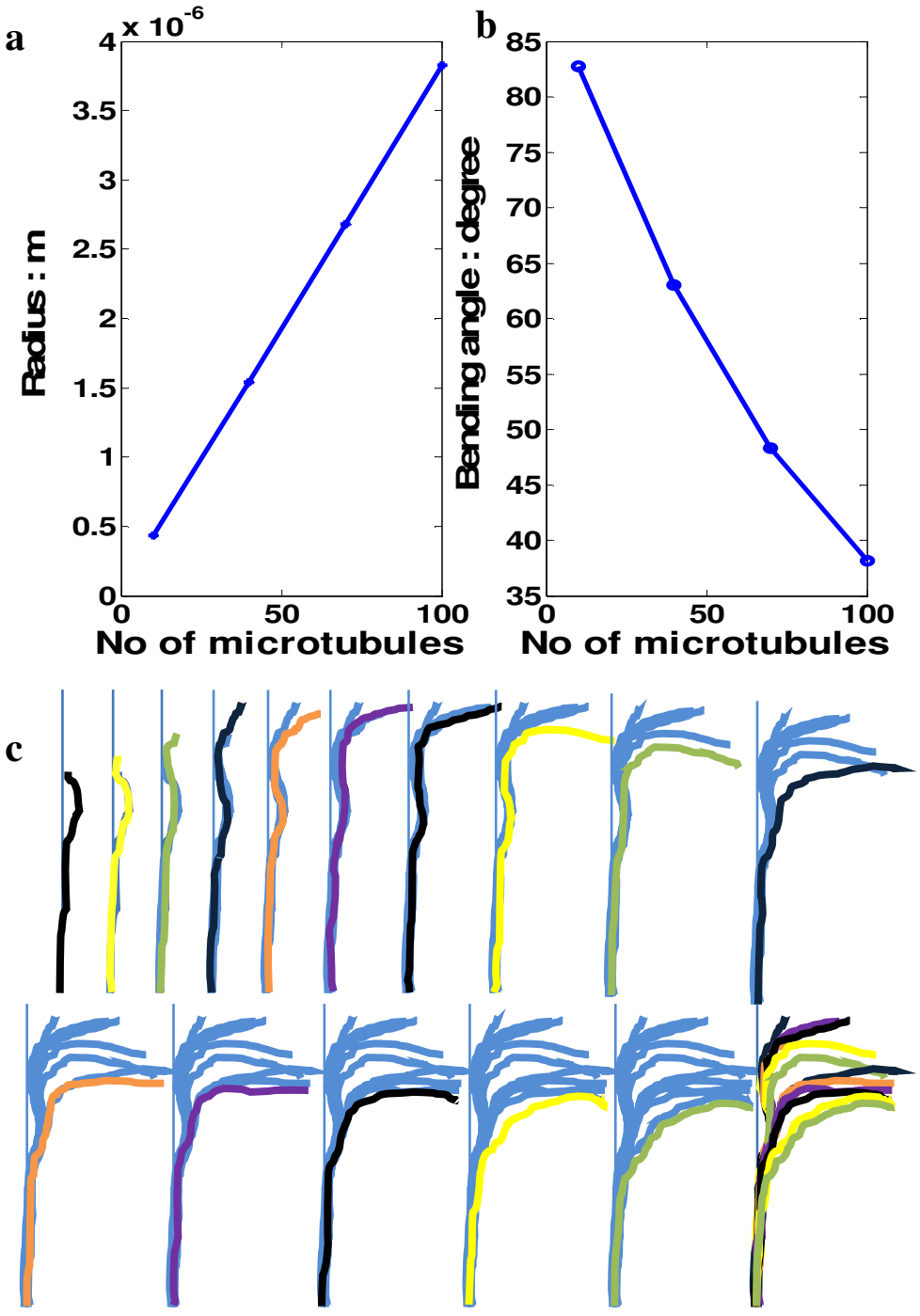

Suppl. Figure 5. (a) Simulation of flow-force induced bending radius as a function of number of microtubules in an axon. (b) Simulated bending angle as a function of number of microtubules for fixed fluid-force. (c) Sequence of overlay profiles depicting the direction of axonal growth with 5 min-intervals.

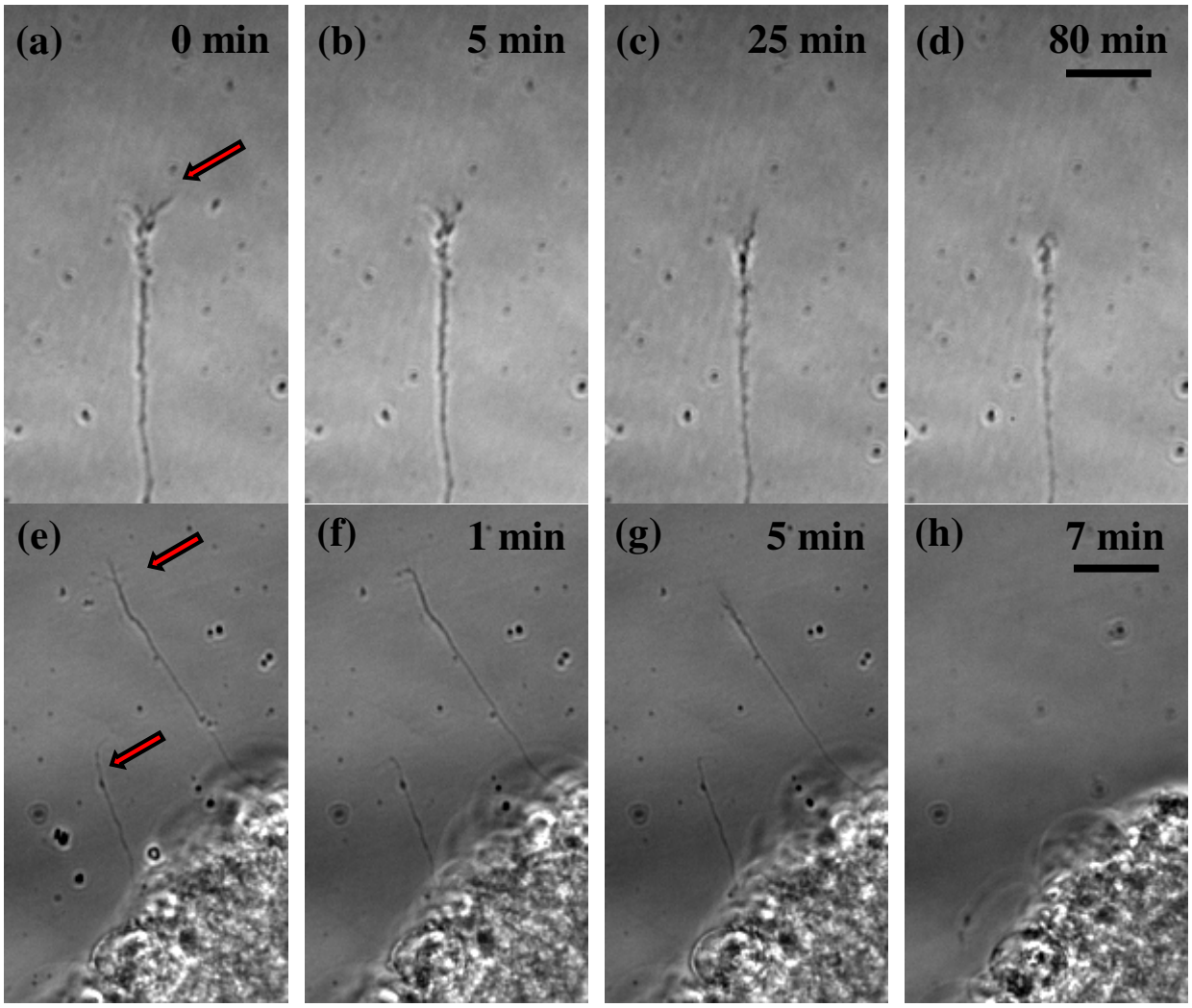

Suppl. Figure 6. (a-d) Slight retraction and no directional response observed due to microfluidic flow. (e-f) Complete detachment of axons due to microfluidic flow. The direction of the fluid flow is indicated by red arrows. All scale bars represent 15 μm.